Eur. Phys. J. A (2025) 61:215
https://doi.org/10.1140/epja/s10050-025-01674-7

THE EUROPEAN PHYSICAL JOURNAL A

Regular Article - Experimental Physics

The CERN n_TOF NEAR station for astrophysics- and application-related neutron activation measurements

The n_TOF Collaboration

N. Patronis[1,2], A. Mengoni[2,3], N. Colonna[4,a], M. Cecchetto[2], J. Lerendegui-Marco[5], O. Aberle[2], C. Domingo-Pardo[5], G. Gervino[6,21], M. E. Stamati[1], S. Goula[1], A. P. Bernardes[2], M. Mastromarco[4,42], A. Manna[7], R. Vlastou[8], C. Massimi[7,40], M. Calviani[2], V. Alcayne[9], S. Altieri[10], S. Amaducci[11], J. Andrzejewski[12], V. Babiano-Suarez[5], M. Bacak[2], J. Balibrea[5], C. Beltrami[10], S. Bennett[13], E. Berthoumieux[14], M. Boromiza[15], D. Bosnar[16], M. Caamaño[17], F. Calviño[18], D. Cano-Ott[9], A. Casanovas[18], F. Cerutti[2], G. Cescutti[19,20], S. Chasapoglou[8], E. Chiaveri[2], P. Colombetti[6,21], P. Console Camprini[7], G. Cortés[18], M. A. Cortés-Giraldo[22], L. Cosentino[11], S. Cristallo[23,24], S. Dellmann[25], M. Di Castro[2], S. Di Maria[26], M. Diakaki[8], M. Dietz[27], R. Dressler[28], E. Dupont[14], I. Durán[17], Z. Eleme[1], S. Fargier[2], B. Fernández[25], B. Fernández-Domínguez[17], P. Finocchiaro[11], S. Fiore[29], V. Furman[30], F. García-Infantes[31], A. Gawlik-Ramiega[12], S. Gilardoni[2], E. González-Romero[9], C. Guerrero[22], F. Gunsing[14], C. Gustavino[31], J. Heyse[33], W. Hillman[12], D. G. Jenkins[34], E. Jericha[35], A. Junghans[36], Y. Kadi[2], K. Kaperoni[8], G. Kaur[14], A. Kimura[37], I. Knapová[38], M. Kokkoris[8], Y. Kopatch[30], M. Krtička[38], N. Kyritsis[8], I. Ladarescu[12], C. Lederer-Woods[39], G. Lerner[2], T. Martínez[9], A. Masi[2], P. Mastinu[41], E. A. Maugeri[28], A. Mazzone[43], E. Mendoza[9], V. Michalopoulou[8], P. M. Milazzo[19], R. Mucciola[23], F. Murtas[44], E. Musacchio-Gonzalez[41], A. Musumarra[45,47], A. Negret[15], A. Pérez de Rada[9], P. Pérez-Maroto[22], J. A. Pavón-Rodríguez[22], M. G. Pellegriti[47], G. Perfetto[42,4], J. Perkowski[12], C. Petrone[15], E. Pirovano[27], J. Plaza[2], S. Pomp[46], I. Porras[31], J. Praena[31], J. M. Quesada[22], R. Reifarth[25], D. Rochman[28], Y. Romanets[26], C. Rubbia[2], A. Sánchez[9], M. Sabaté-Gilarte[2], P. Schillebeeckx[33], D. Schumann[28], A. Sekhar[13], A. G. Smith[13], N. V. Sosnin[39], A. Sturniolo[6], G. Tagliente[4], A. Tarifeño Saldivia[5], D. Tarrío[46], P. Torres-Sánchez[31], S. Urlass[36], E. Vagena[1], S. Valenta[38], V. Variale[4], P. Vaz[26], G. Vecchio[11], D. Vescovi[25], V. Vlachoudis[2], T. Wallner[36], P. J. Woods[39], T. Wright[13], R. Zarrella[40], P. Žugec[16]

[1] University of Ioannina, Ioannina, Greece
[2] CERN, Geneva, Switzerland
[3] ENEA, Bologna, Italy
[4] INFN, Sez. di Bari, Bari, Italy
[5] Instituto de Física Corpuscular, CSIC, Universidad de Valencia, Valencia, Spain
[6] Dipartimento di Fisica, Università di Torino, Turin, Italy
[7] INFN, Sez. di Bologna, Bologna, Italy
[8] National Technical University of Athens, Athens, Greece
[9] Centro de Investigaciones Energéticas Medioambientales y Tecnológicas (CIEMAT), Madrid, Spain
[10] INFN and Università di Pavia, Pavia, Italy
[11] INFN, Laboratori Nazionali del Sud, Catania, Italy
[12] University of Lodz, Lodz, Poland
[13] University of Manchester, Manchester, United Kingdom
[14] CEA Irfu, Université Paris-Saclay, 91191 Gif-sur-Yvette, France
[15] Horia Hulubei National Institute of Physics and Nuclear Engineering, Măgurele, Romania
[16] Department of Physics, Faculty of Science, University of Zagreb, Zagreb, Croatia
[17] University of Santiago de Compostela, Santiago, Spain
[18] Universitat Politècnica de Catalunya, Terrassa, Spain
[19] INFN, Sez. di Trieste, Trieste, Italy
[20] INAF, Osservatorio Astronomico di Trieste, Trieste, Italy
[21] INFN, Sez. di Torino, Turin, Italy
[22] Universidad de Sevilla, Seville, Spain
[23] INFN, Sez. di Perugia, Perugia, Italy
[24] INAF, Osservatorio Astronomico di Teramo, Teramo, Italy
[25] Goethe University, Frankfurt, Germany
[26] Instituto Superior Técnico, Lisbon, Portugal
[27] Physikalisch-Technische Bundesanstalt (PTB), Bundesallee 100, 38116 Braunschweig, Germany
[28] Paul Scherrer Institut (PSI), Villigen, Switzerland

Published online: 23 September 2025

[29] ENEA, Frascati, Italy
[30] Joint Institute for Nuclear Research (JINR), Dubna, Russia
[31] University of Granada, Granada, Spain
[32] INFN, Sez. di Roma, Rome, Italy
[33] European Commission, Joint Research Centre (JRC), Geel, Belgium
[34] University of York, York, United Kingdom
[35] TU Wien, Atominstitut, Stadionallee 2, 1020 Wien, Austria
[36] Helmholtz-Zentrum Dresden-Rossendorf, Dresden, Germany
[37] Japan Atomic Energy Agency (JAEA), Tokai-Mura, Japan
[38] Charles University, Prague, Czech Republic
[39] School of Physics and Astronomy, University of Edinburgh, Edinburgh, United Kingdom
[40] Dip. Fisica e Astronomia, Università di Bologna, Bologna, Italy
[41] INFN, Laboratori Nazionali Legnaro, Legnaro, Italy
[42] Dip. Interateneo di Fisica, Università di Bari, Bari, Italy
[43] CNR, Bari, Bari, Italy
[44] INFN, Laboratori Nazionali di Frascati, Frascati, Italy
[45] Department of Physics and Astronomy, University of Catania, Catania, Italy
[46] Uppsala University, Uppsala, Sweden
[47] Istituto Nazionale Fisica Nucleare, Sez. di Catania, Catania, Italy

Received: 14 March 2025 / Accepted: 25 August 2025

Communicated by Jose Benlliure

Abstract A new experimental area, the NEAR station, has recently been built at the CERN n_TOF facility, at a short distance from the spallation target (3 m). The new area, characterized by a neutron beam of very high flux, has been designed with the purpose of performing activation measurements of interest for astrophysics and various applications. The beam is transported from the spallation target to the NEAR station through a hole in the shielding wall of the target, inside which a collimator is inserted. The new area is complemented with a γ-ray spectroscopy laboratory, the GEAR station, equipped with a high-efficiency HPGe detector, for the measurement of the activity resulting from irradiation of a sample in the NEAR station. The use of a moderator/filter assembly is envisaged, in order to produce a neutron beam with quasi-Maxwellian energy distribution, of different thermal energies, necessary for the determination of Maxwellian Averaged Cross Sections of astrophysical interest. A new fast-cycling activation technique is also being investigated for measurements of reactions leading to isotopes of very short half life.

1 Introduction

Neutron-induced reactions play an important role in a variety of fields in Fundamental and Applied Nuclear Physics. In nuclear astrophysics, neutron capture reactions and β-decay are responsible for the synthesis of all elements from iron up to uranium in the Universe, in two main stellar scenarios, each being responsible for the production of about one half of the observed elemental abundances. The slow neutron capture process (or *s* process in short), occurs during the advanced burning phases of stellar evolution [1,2]. Depending on the stellar mass, the *s* process operates in thermally pulsing low-mass Asymptotic Giant Branch (AGB) stars (main component) [3] or during core He and shell C burning in massive stars (weak component) [4]. Rapid neutron capture, or *r* process [1], occurs in explosive scenarios and leads to the production of short-lived and very neutron-rich nuclei, which later decay to the known stable isotopes. Recent works suggest that a likely source of *r*-process elements could be the catastrophic aftermath of neutron star mergers, particularly the material ejected during and after the merger. Some core-collapse supernovae, especially those with strong magnetic fields or peculiar conditions leading to neutron-rich ejecta, also remain as potential sites, though perhaps for a subset of r-process elements (see e.g. [5–7]).

The main features of the chemical evolution of the Universe and of heavy element production are reasonably well described by stellar models incorporating the two neutron capture processes mentioned above. To this end, accurate stellar cross sections are a fundamental input in order to reproduce the observed abundances. At present, the knowledge of neutron cross sections is still unsatisfactory for several isotopes. Sensitivity studies based on state-of-the-art models for massive stars [8] and thermally pulsing AGB stars [9] indicate that the cross sections of numerous isotopes need to be re-measured with greater accuracy or over more comprehensive neutron-energy ranges in order to derive reliable astrophysical information and further refine details of such

[a] e-mail: nicola.colonna@ba.infn.it (corresponding author)

models. Recent discussions about the key isotopes and the main challenges in the field are provided in Refs. [10–12].

Neutron-induced reactions play a key role also in a variety of applications related to the fields of energy, nuclear medicine, material studies, as well as reactor, environmental and space dosimetry. In particular, data on neutron capture and neutron-induced fission reactions are important for improving the performance and safety operation of current fission reactors or for the design of future generation ones, including systems for nuclear waste incineration [13]. In nuclear medicine, neutron-induced reactions are at the basis of the production of a number of radioisotopes for diagnosis and therapy, and the knowledge of the cross section for a series of neutron reactions in biological tissues is fundamental for an accurate dose estimate in radiotherapy.

Neutron cross section data are also needed for the lifetime assessment of fusion reactors now being developed [14]. As an example, integral cross sections are required for a number of elements (or specific isotopes) for the estimate of the radiation damage in structural material of the reactors. In particular, integral cross sections for both transmutation and neutron-induced charged-particle reactions are needed to estimate neutron damage effects in the inner components of the reactors, related to the variation of the chemical composition of the material and/or to gas production [15]. Activation cross sections, mostly related to neutron capture reactions, are also needed to address safety, licensing, decommissioning, and waste management issues of future fusion systems [16]. At present, cross section data in this respect are either missing or unreliable for several critical isotopes, both below and above 14 MeV, the energy of neutrons produced in D-T generators. The request of data for fast neutrons (i.e. with kinetic energy from a few MeV to a few tens of MeV) is related to material studies at future neutron irradiation facilities, such as IFMIF and its precursor DONES [17], characterized by neutron spectra that extend up to several tens of MeV. As in the case of astrophysics-related requests, the lack of data is a direct consequence of the lack of suitable neutron facilities, in terms of energy range and flux of the beam, as well as of the typically low cross section ($\sim 10\,\mu$b) and/or unavailability of isotopically pure samples.

Energy-dependent cross section of neutron-induced reactions relevant to nuclear astrophysics and applications have been measured for more than two decades at the n_TOF facility at CERN [18] by the time-of-flight technique. However, the intrinsic limitations of the technique, in terms of signal-to-background ratio, has hindered much-needed measurements for a number of important isotopes, in particular short-lived ones, and for specific reaction channels.

To overcome such limitations, a new experimental area, the NEAR station, set at a very short distance of a few meters from the spallation source, has recently been proposed and constructed at n_TOF during the long CERN accelerator shut down (2019–2021). A detailed description of this newly built area is given in Ref. [19], while some physics cases are discussed in [20]. The purpose of this work is to present the main features of the neutron beam in the NEAR station and its capabilities with respect to the implementation of the activation technique. The new experimental area is complemented by a dedicated laboratory, referred to as the GEAR station (Gamma spectroscopy Experimental ARea), currently equipped with a HPGe detector for γ-ray spectroscopy.

The new high-flux irradiation station for activation measurements (the a-NEAR station hereafter) will allow the n_TOF Collaboration to fully exploit the sensitivity and the selectivity of the activation technique. This will make feasible measurements of neutron activation cross section for reactions that until now have been outside the possibilities of the n_TOF facillity, thus experimentally accessing previously unexplored physics cases.

Specifically, by means of a neutron moderator/filter system, quasi-Maxwellian neutron spectra could be produced to be used for measurements of Maxwellian Averaged Cross Sections (MACS) at different stellar temperatures on unstable and low mass samples, or for cases in which extremely low reaction rates are expected. Additionally, concerning future plans, the CERN-PS proton pulse time structure (one pulse every 1.2 s) may allow the implementation of the fast cyclic activation technique [21].

In this paper we present the main features of the newly completed a-NEAR station, the basic parameters of the neutron beam inside the area, the laboratory for activity measurement, and new measurement capabilities currently being investigated. The paper is organized as follows: in Sect. 2 the a-NEAR station is described. The main features of the neutron beam in terms of neutron spectrum, flux and spatial profile, provided by Monte Carlo simulations are presented in Sect. 3. The γ-ray spectroscopy laboratory for activity measurement (GEAR) is discussed in Sect. 4. Section 5 then presents two techniques now being investigated for astrophysics-related measurements. Conclusions and perspectives are finally given in Sect. 6.

2 The NEAR experimental area

Recently, the n_TOF facility has undergone major upgrades. We remind here that neutrons at n_TOF are produced by spallation reactions induced by 20 GeV/c protons, in pulses of 7×10^{12} protons, 7 ns (rms) width, and maximum repetition rate of 0.8 Hz, delivered by the CERN Proton Synchrotron (PS), impinging on a massive lead target. During CERN's Long Shutdown period of 2019–2021, the target pit shielding has been completely overhauled and a new generation spallation target has been installed [22].

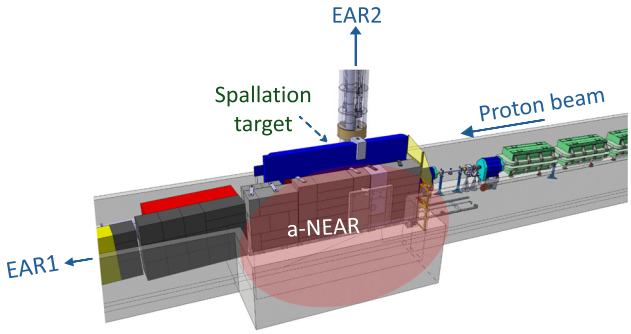

Fig. 1 A schematic view of the n_TOF spallation target area, the proton beam line, the two neutron beam lines for time-of-flight measurements, and of the a-NEAR station

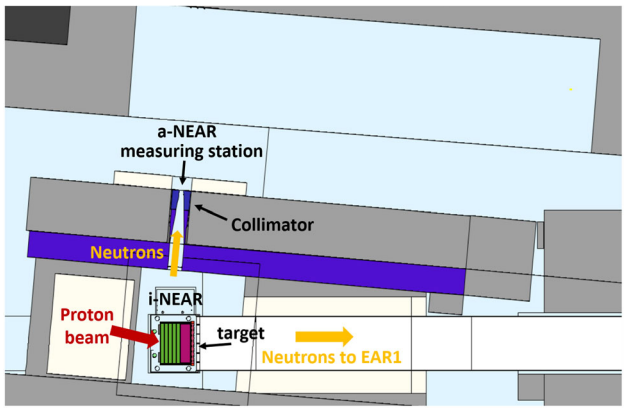

Fig. 2 The NEAR Station schematic design (top view), as implemented in simulations of the n_TOF facility

Taking advantage of the consolidation work on the n_TOF target area, a new experimental station, generically referred to as the 'NEAR' station (because of its vicinity to the spallation target), has been constructed. The main purpose of this new installation is to exploit the extremely high neutron intensity close to the target in order to perform challenging activation measurements as well as to study radiation damage on non-metallic materials [23].

The NEAR station comprises two areas, the Irradiation area (indicated as i-NEAR) and the Activation area (a-NEAR), with the first one positioned directly next to the spallation target and the second one located outside the target pit shielding, at a distance of 3 m from the target center. The details of i-NEAR can be found in [19]. Briefly, this station is used for studying neutron damage to polymeric material whose radiation resistance goes from a few kGy to a few MGy, with the damage consisting essentially on the breaking of molecular bonds. On the contrary, it cannot be used for metallic materials, for which the damage is essentially due to the production of vacancies and defects in the lattice structure of the metal, which requires a threshold dose level (from a few GGy up) approximately three orders of magnitude higher than available at i-NEAR. This paper focuses on the features and applications of the a-NEAR. A schematic design of the spallation target area of the n_TOF facility, with the location of the a-NEAR station can be seen in Fig. 1. The a-NEAR experimental area is located just outside the shielding wall on the left side of the n_TOF neutron spallation target (as seen from the proton beam). The shielding is made of 40 cm thick cast iron wall followed by 80 cm thick concrete wall (shown as blue and gray walls, respectively, in Fig. 2). Finally, around the neutron beam exit an additional 20 cm thick marble shielding is present (white wall in Fig. 2). Being essentially made of calcium carbonate, marble is little affected by neutron activation, and can therefore conveniently be used as the last shielding part in collimation systems for neutron beams, to minimize γ-ray ambient background. The bunker has a rectangular shape, 7 m long, 2.6 m wide and 2.8 m tall. The neutron beam is transported through a 26 cm diameter hole in the shielding wall, at 1.2 m from the floor, specifically designed to house a collimation system. The collimator is 80 cm long and is placed just inside the middle section of the shielding wall (made of concrete). It has a conical shape, with an entrance and exit holes of 25 and 6 cm diameter, respectively. The first 50 cm are made of stainless steel, while the remaining 30 cm are made of a series of borated polyethylene disks.

A photo of the collimator exit face is shown in Fig. 3, along with a sample holder used for activation measurements. Neutron irradiation can be performed at the exit of the collimator (position A in the photo), or just outside the marble wall (position B), at 20 cm distance from the exit hole of the collimator, inside the a-NEAR bunker. The neutron beam is dumped on the wall opposite the collimator exit, where irradiation of additional material (such as electronic devices) can be performed. The neutron beam collimation system points to the side of the target (orthogonal to the proton beam direction). As a consequence, the very high energy component of the neutron beam is absent. An additional moderation of the neutron beam can be performed by placing a block of suitable moderating material close to the target. In this respect, a shelf for housing such a moderator has been designed and implemented on the structure currently used for material irradiation studies (see Fig. 6 in Ref. [19]). The importance of the moderator, together with a low-energy filter, is discussed in Sect. 5.1.

One of the advantages of the a-NEAR station is that irradiation with the neutron beam can be performed parasitically, i.e. without disturbing experiments simultaneously performed in the other two experimental areas of n_TOF (EAR1 at the end of a 185 m long horizontal beam line and EAR2 at the end of a 19 m long vertical beam line). The main advantage of NEAR, however, is the very high neutron flux, a direct consequence of the short distance from the spalla-

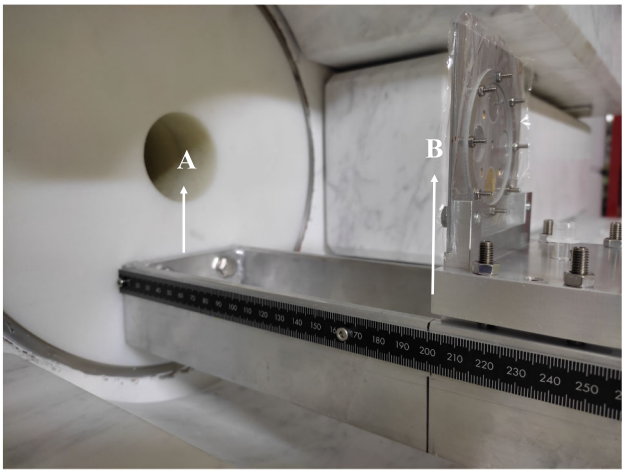

Fig. 3 The neutron irradiation position as seen from inside the a-NEAR bunker. The photo shows the collimator exit surface and the last part of the shielding wall, made of marble. Letters A and B denote the two irradiation positions discussed in the text. The photo also shows a multi-foil sample holder used for the commissioning of the a-NEAR neutron beam, mounted on a rail in the irradiation position B, at 20 cm distance from the collimator exit surface

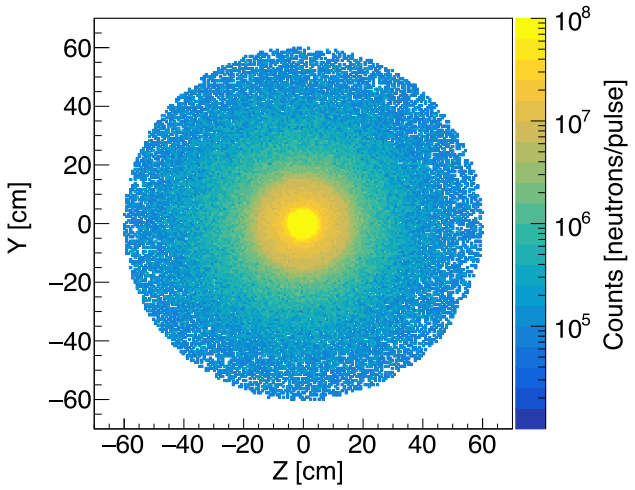

Fig. 4 Spatial distribution of the neutron beam on the external marble surface (position "B"), within 60 cm of radius from the center of the collimator

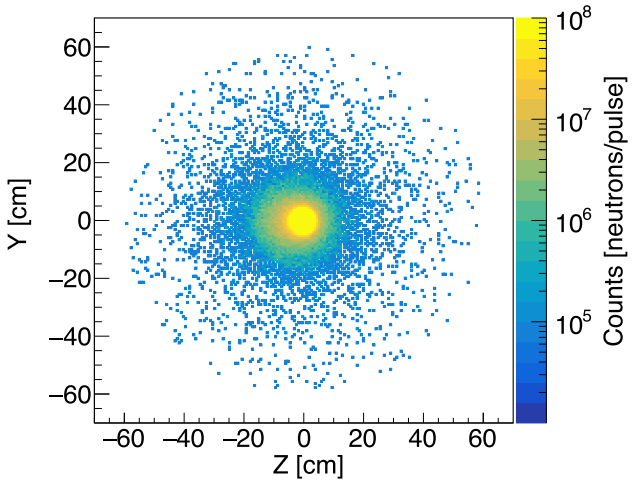

Fig. 5 2D distribution of neutrons crossing the scoring surface on the external marble surface (position "B") with an angle within 10 degrees relative to the normal

tion target. In the following, the main features of the neutron beam, determined by means of Monte Carlo simulations, are presented.

3 The a-NEAR neutron beam

FLUKA Monte Carlo simulations [24–26] were carried out to characterize the area around the collimator, in terms of particle fluence and dose level. The neutron 2D spatial distribution was recorded in two positions: right at the exit of the collimator (hereafter denoted as position "A"), and at a distance of 20 cm from the exit face of the collimator, aligned with the external surface of the marble shielding (denoted as position "B").

According to simulations, the latter position (B) represents the best compromise between beam dimension and neutron background, and therefore is planned to be used for the irradiation of most of the samples. In the simulations, neutrons are transported from the side face of the spallation target through the collimator and the shielding wall, and recorded on a scoring surface of 60 cm radius. The resulting beam spatial profile is shown in Fig. 4. The plot shows the neutrons crossing the scoring surface from all directions, normalized to the nominal proton pulse (one pulse corresponding to 7×10^{12} protons). Secondary hadrons other than neutrons (i.e. protons, muons, etc.) exiting the collimator amount to less than 0.3% of the total number of particle crossing the scoring surface.

Figure 5 shows the neutron distribution on the same surface as for Fig. 4, but considering only neutrons impinging within an angle of 10 degrees with respect to the normal to the scoring surface. As can be seen, the distribution is not symmetric anymore with respect to the collimator center and presents a higher flux on one side of the collimator hole. The shift is due to the geometry of the collimator with respect to the target, with the collimator axis not perfectly perpendicular to the target surface, being tilted by 5 degrees. This effect is not evident in Fig. 4, where no condition is applied on the crossing angle, probably because of the contribution of neutrons scattered around the collimator and shielding.

Figure 6 shows the projection of the neutron beam profile on the horizontal direction (z) along the exit face of the collimator. From the figure it can be appreciated that the neutron flux is as high as 9×10^8 n/cm^2/pulse within ± 5 cm from the center of the collimator. The figure also shows that outside the collimator hole, a tail of neutrons is present, mostly pro-

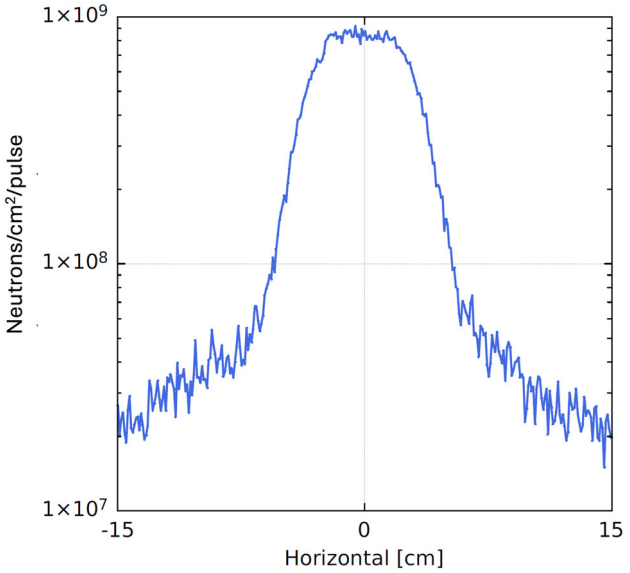

Fig. 6 Projection of the neutron beam profile on the horizontal direction at the external marble surface (position "B").

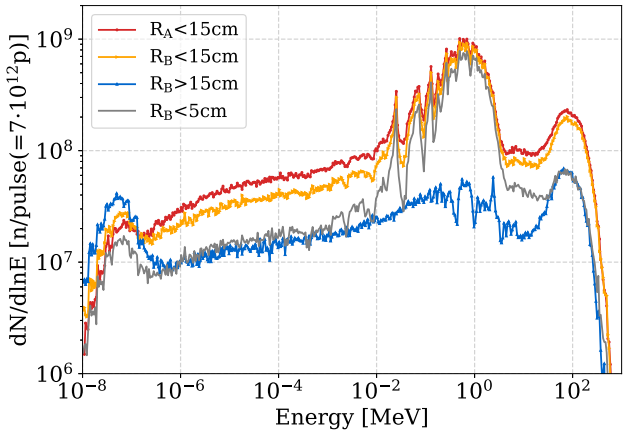

Fig. 7 Comparison of neutron spectra (in units of lethargy and per proton pulse) at the exit of the collimator hole (position A), and at the external surface of the marble shielding (position B), within different distances from the collimator center.

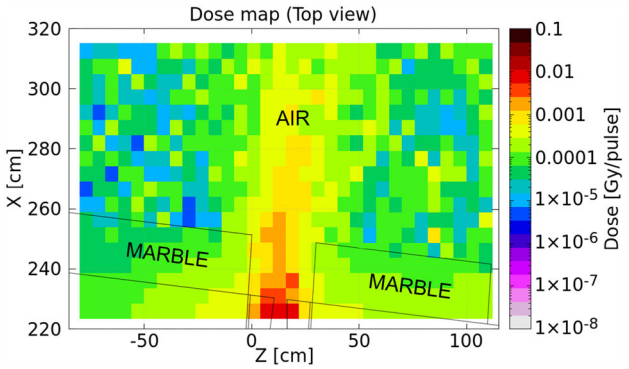

Fig. 8 Dose map overview at the exit of the collimator and in the bunker (see text for details). The Z = 0 position corresponds to the center of the spallation target

duced by neutrons scattered inside the collimator itself or in the shielding wall.

Figure 7 shows the simulated neutron spectra for different conditions on the beam profile (shown in Fig. 4). Specifically, the condition is applied on the radius R_B from the collimator center, at the marble surface (position "B"). For instance, the spectrum denoted as $R_B < 15$ cm includes only neutrons recorded on the scoring surface within 15 cm distance from the collimator center. It should be noticed that the spectra are shown in units of counts (per pulse) to allow a direct comparison, hence, they are not normalized per unit surface. For comparison, the spectrum on the internal marble surface (position "A") is also shown in the figure, at a distance from the collimator center $R_A < 15$ cm. The comparison indicates that the neutron flux at that position is slightly higher than the one on the surface B, for the same radius, as expected from beam divergence considerations.

Another consideration regards the spectrum of neutrons recorded in the position B "outside" the collimator, i.e. at a distance from the collimator center greater than 15 cm ($R_B >$ 15 cm). Such neutrons are at least partially traversing the marble shielding and represent a source of background both inside and outside the neutron beam. It can clearly be seen in Fig. 7 that neutrons of energy above ~0.2 eV are strongly attenuated, while on the contrary the thermal neutron flux is higher because of the thermalization of fast neutrons when passing through the shielding.

The total ionising dose level predicted by the simulations around the exit of the collimator and in the bunker, averaged in a 30 cm wide horizontal plane centered on the collimator is shown in Fig. 8. The meaningful information in this plot is the dose in air, as the marble is part of the shielding wall and it is therefore inaccessible. The dose values in air in the proximity of the collimator exit face are around 1–2 mGy/pulse. This relatively large value implies that it may be difficult to operate detectors (either active or passive ones) in the vicinity of the collimator, unless they are characterized by a high radiation tolerance or are very carefully shielded. The figure also indicates that, like for neutrons, photons as well exit the collimator slightly shifted to one side with respect to the center.

4 The GEAR station

Activation measurements at n_TOF are carried out in two steps. In the first one, the sample is irradiated with the neutron beam in the a-NEAR station, right outside the shielding wall (see Fig. 3). The second step of the activation technique consists in the accurate measurement of the induced sample

Fig. 9 The HPGe-based γ-ray spectrometer, placed in the GEAR Station. The detector is inside the lead shielding shown in the photo, while the refrigeration and front-end electronics are located underneath the shielding

Fig. 10 Left panel: A view from the top of the HPGe detector inside the lead shield. Right panel: same as before, but with the polyethylene sample holder on top of the detector

activity. To this end, the n_TOF Collaboration has established a dedicated experimental facility, the GEAR station, situated within the premises of the n_TOF facility at CERN. The GEAR station is situated approximately 240 m from the lead spallation target and is located in an underground area. The low radiation background conditions and the fact that this is a radiation-controlled area enable the safe handling of irradiated samples.

The GEAR station is equipped with a CANBERRA HPGe detector GR5522. Photos of the setup are shown in Figs. 9 and 10. The detector is an n-type HPGe detector of 63% relative efficiency. This feature, combined with a very thin carbon end cap composite window, enables high efficiency measurements of γ-rays with energies from 3 keV up, considerably pushing down the low energy limit relative to standard windows. The energy resolution of the detector is 3 keV at 1.33 MeV γ-ray energy, with a peak-to-Compton ratio of 64:1. The preamplifier circuit of this detector is equipped with a suitably designed fast-switch circuit [27] that makes possible to use the detector also for time-of-flight measurements close to the neutron beam line in the other two n_TOF experimental areas (EAR1 and EAR2) where a large prompt signal, or γ-flash, is present. The detector is cooled by means of the CANBERRA CP-5 electrically refrigerated cryostat for continuous and safe operation of the HPGe detector in cases where large volume liquid nitrogen dewars have to be avoided (in particular in underground areas with limited space). The performance of an electrically refrigerated device is similar to the one of a liquid-nitrogen cooled HPGe.

For optimal background conditions, the HPGe device is placed inside the 747 CANBERRA lead shield, as shown in Fig. 9. The interior of the 747 CANBERRA lead shield is coated with 1 mm tin layer and 1.6 mm copper layer to prevent interference with lead X-rays. The HPGe detector, inside the lead shield, is shown in the left panel of Fig. 10.

Measurements of the activity of the irradiated samples can be performed at different source-to-detector distances, ranging from 0 to 25 cm, thanks to a suitably designed system made of different polyethylene spacers and sample holders that can be stacked one on top of the other. A picture of such a system, mounted on the detector, is shown in the right panel of Fig. 10. The versatile detection geometry is of great help for high-accuracy measurements, as it allows one to choose the optimal configuration depending on the expected counting rate. As the detection geometry determines the efficiency, its reproducibility significantly affects the accuracy of the experimental results. Thanks to the spacers system the distance between the sample and the detector window can be reproduced with an accuracy better than 0.1 mm.

The most important requisites for high-accuracy measurements of the activity are a low background and a reliable knowledge of the detector efficiency as a function of the γ-ray energy. Figure 11, top panel, shows the background measured for a threshold on the amplitude corresponding to a deposited γ-ray energy of 63 keV. As evident, only the typical room background γ-ray spectrum is recorded, due to the strategic positioning of the GEAR station which is situated at a considerable distance and effectively shielded from the lead spallation target and other intense sources of radioactiv-

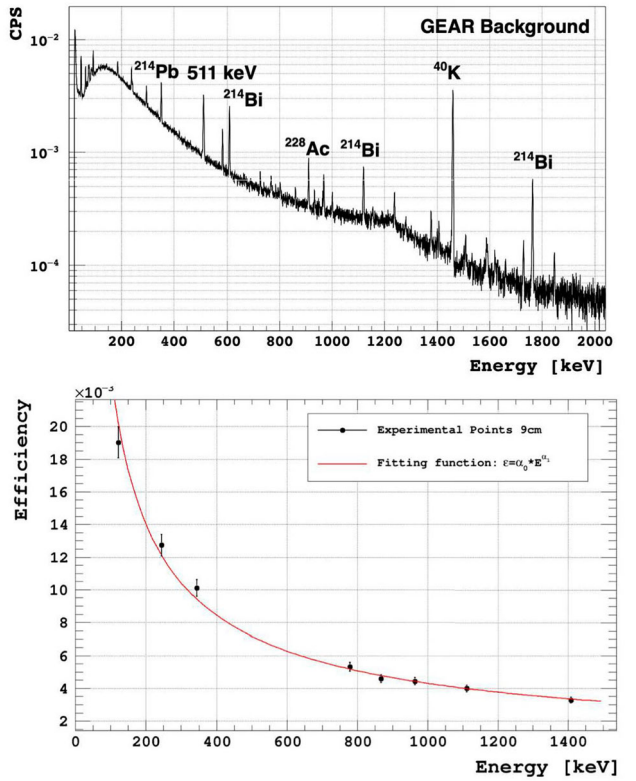

Fig. 11 Top panel: The background of the HPGe detector in the GEAR station. Bottom panel: The efficiency of the γ-ray spectrometer, as obtained using a ^{152}Eu calibrated point source at a 9 cm distance. The red curve represents a fit of the measured efficiencies with a power law, used for interpolation purposes

ity. The efficiency is determined by means of several calibration γ-ray sources, whose activity is known to within 1–2% accuracy. The bottom panel of Fig. 11 shows the efficiency measured with a ^{152}Eu calibrated point-like source, at a distance from the detector of 9 cm. For interpolation purposes, the measured efficiency was fitted with a simple power law shown by the red curve in Fig. 11. This efficiency curve serves primarily as an illustration to demonstrate the capabilities of the detector. In actual γ-ray measurements, the detection efficiency for each gamma-ray energy is determined through extensive GEANT4 simulations. These simulations meticulously consider the decay scheme, sample geometry, and the adopted detection geometry. Consequently, potential summing effects, γ-ray attenuation effects, and extended sample geometry efficiency corrections are systematically deduced through GEANT4 simulations that have undergone rigorous validation using point-like calibrated sources at various source to detector window distances.

The setup can be adapted to include a cylindrical BC408 plastic scintillator of 4 cm diameter and 10 mm thickness, which is commonly used for β-only emitters. In this setup, the irradiated sample can be positioned in very close proximity to the plastic detectors, ensuring at the same time optimal geometry with respect to the HPGe detector. This arrangement facilitates the utilization of β-γ coincidence measurements, which can further enhance the signal-to-background ratio compared to the "singles" γ-ray measurement.

For the GEAR station two Data Acquisition systems are available. When standard single measurements are performed, a system based on Mirion model 2026 amplifier and an Amptek MCA-8000D digital mltichannel analyzer is used. Additionally, a fully digital DAQ system is available based on the CAEN DT 5730S 500MS/s 8-channel digitizer. The digital DAQ extends significantly the flexibility of data analysis modes (singles or coincidences) by recording the full waveform of the signals from the HPGe preamplifier and the anode signal of the plastic scintillator photomultiplier tube.

5 New measurement capabilities and perspectives

In this section we present two examples of activation measurements that can be performed at the a-NEAR station. Both cases are mostly relevant for an experimental program on nuclear astrophysics, but the use of beam-shaping techniques and innovative instrumentation could make feasible challenging measurements of interest for other fields as well, in particular relevant for fusion technologies or for nuclear medicine.

5.1 Beam filtering for astrophysics-related measurements

One of the most important nuclear data needs for the understanding and modelling of stellar nucleosynthesis is the Maxwellian Averaged Cross Section of neutron capture reactions for various thermal energies kT, ranging from a few to a few hundred keV. Two methods are typically used to experimentally determine this quantity: (i) measure the energy-dependent reaction cross section (using the time-of-flight technique) and subsequently calculate the MACS by performing a spectral averaging using a Maxwellian spectrum of the desired temperature; (ii) measure the integral cross section by activation with a neutron beam with quasi-Maxwellian spectrum. While the latter method is typically used at neutron facilities based on low-energy accelerators [28–30], at n_TOF all MACS of astrophysical interest have so far been obtained from time-of-flight measurements. As already mentioned, however, the limited sensitivity of the time-of-flight technique has up to now hindered the possibility to investigate some challenging reactions, in particular on short-lived radionuclides. Whenever applicable, the highly-sensitive activation technique can enable access to isotopes available in very small quantities, as small as a few ng, that are difficult to access in a TOF experiment. The construction of the NEAR station has opened the possibility to directly measure at n_TOF the MACS for different kT, by means

of the activation technique. To this end, the neutron spectrum has to be suitably shaped so to resemble a Maxwellian distribution. This can be achieved by means of a moderation system, needed in particular to suppress the high-energy component, followed by a filtering setup to suppress the low-energy component. The former has to be placed right next to the spallation target, while the latter can be installed in the a-NEAR station, just downstream of the collimator. Different choices of the moderation material are now being investigated, for different applications. A reasonable reproduction of a Maxwellian spectrum that still preserves a high flux can be obtained with a moderator of suitable material and dimension. Analytical calculations, confirmed by detailed Monte Carlo simulations performed with the GEANT4 toolkit (described below), show that indeed a reasonable shaping of the neutron spectrum can be achieved by using an AlF_3 moderator, encapsulated in an Al casing and placed at direct contact with the spallation target, coupled to a boron carbide (B_4C) filter, with 95%-enriched ^{10}B, surrounding the activation sample. Quasi-Maxwellian neutron spectra corresponding to different kT can be obtained simply by varying the thickness of the ^{10}B-based filter.

Figure 12 shows the effect of 95% enriched ^{10}B filters of different thicknesses, combined with an AlF_3 moderator 20 cm thick. For each filter thickness, a comparison is shown of the simulated a-NEAR spectrum with a Maxwell–Boltzman distribution at the kT best fitting the spectrum. The similarity between the two spectra is evident for stellar temperatures typical of s-process nucleosynthesis. Calculations indicate that MACS at different kT can be determined with a reasonable accuracy by the activation technique in the a-NEAR station, up to about kT=100 keV, by measuring the NS-SACS of a given isotope relative to the one of the standard $^{197}Au(n,\gamma)$ reaction, used for normalization purposes. Figure 13 provides some indication on the uncertainty related to the use of the technique described above for MACS determination. For each isotope, the figure shows the ratio between the Spectral Averaged Cross Sections (SACS) calculated by convoluting the evaluated cross section with the true Maxwellian distribution at kT = 25 keV (M-SACS) and the quasi-Maxwellian neutron spectrum in the a-NEAR station (NS-SACS), normalized to the same ratio calculated for the $^{197}Au(n,\gamma)$ cross section. It can be seen that the ratio is on average close to 1, with differences of the order of 10–15%, except for the lightest isotopes. This value can therefore be assumed as a realistic estimate of the most probable uncertainty in the MACS that would be determined in a measurement at the a-NEAR station for any isotope of unknown capture cross section.

The use of a moderator to suppress or reduce the high-energy neutron component may not be strictly necessary in (n,γ) activation measurements, since high-energy neutrons (E_n >1 MeV) do not contribute significantly to the MACS, due to the typically negligible value of the capture cross sec-

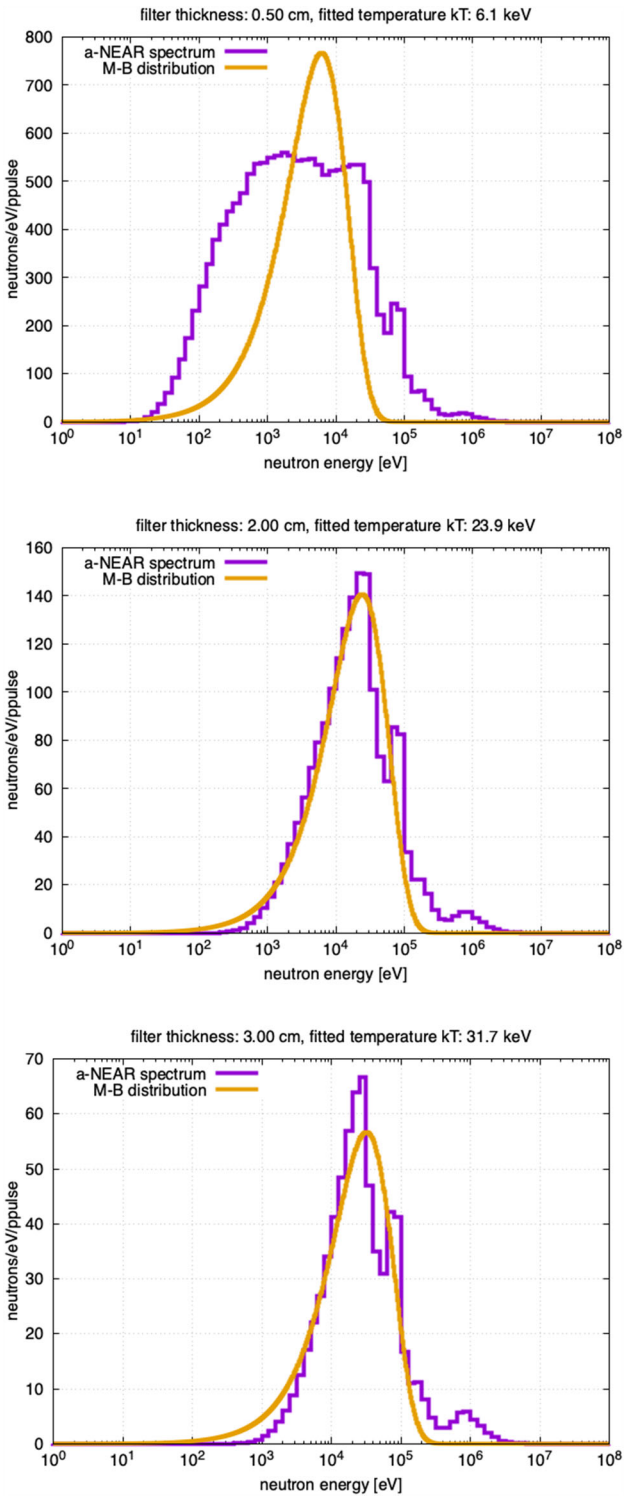

Fig. 12 The simulated neutron spectrum in the a-NEAR station, obtained with the use of an AlF_3 moderator of 40 kg mass, mounted next to the spallation target and a ^{10}B-based filtering system placed at the exit of the collimator (purple histogram). The different panels show the spectrum for increasing filter thickness (from top to bottom). For comparison, the yellow curve shows the Maxwell–Boltzmann distribution at kT (shown in the legend), that best fits the a-NEAR spectrum

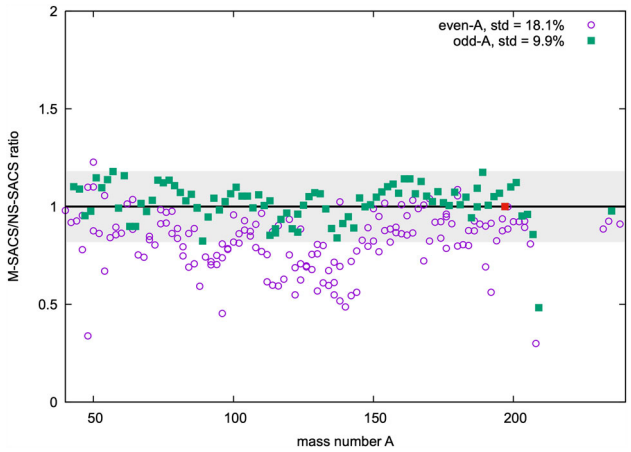

Fig. 13 Ratio between the M-SACS at kT = 25 keV and the SACS calculated with the neutron beam of the a-Near Station (NS-SACS), normalized to the calculated ratio for ^{197}Au, for stable nuclei with A > 40. In all cases the capture cross section from ENDF/B-VIII was used. The neutron spectrum in a-NEAR is obtained with a 20 cm thick AlF_3 moderator plus 3 cm thick 95% enriched ^{10}B filter). The standard deviation for all-A nuclei is 18.2%

tion at high neutron energies. A filtering system alone could therefore be enough for measurements of the MACS, at least in a limited kT range. Such an option is now being investigated, both with simulations and experimentally. The neutron energy distribution at the irradiation position can be estimated by means of Monte Carlo simulations, performed with the GEANT4 toolkit, assuming a sample placed in the center of a cylinder made of 95% ^{10}B enriched boron carbide (B_4C). Neutrons in the thermal and epithermal energy regions are moderated and eventually absorbed by the B_4C cylinder, producing a peak in the keV region that resembles a Maxwellian distribution, plus a tail at high energy (see Fig. 6 of Ref. [20]) that, however, does not contribute significantly to the SACS. While some information on the MACS can be obtained in this way, an upgrade of the NEAR station is already planned, with the installation of a moderator inside the spallation target pit, in order to improve the agreement between the filtered and expected Maxwell-Boltzmann distributions.

5.2 The CYCLING station

The high neutron flux at a-NEAR opens the way to challenging (n,γ) activation measurements on extremely small mass samples and/or on short-lived isotopes. Typically, samples are irradiated for several days to weeks at a-NEAR and transported to and measured in the GEAR station described in Sect. 4. This activation scheme is well suited for (n,γ) measurements with long-lived product isotopes ($t_{1/2} \geq$ several hours). However, it imposes an intrinsic limit on the accessible physics cases, specifically on the minimum half-life of the (n,γ) product, given by the time one has to wait (for radioprotection reasons) before entering the a-NEAR bunker and for transporting the sample to the offline detector. This limitation can be overcome with the installation of a cyclic activation station for (n,γ) experiments (CYCLING). This setup would enable the repetition of a short irradiation, rapid transport to a detector, measurement of the decay and transport back to the irradiation position. Depending on the duration of the transport of the sample to the detector, half-lives of the activated nuclei of order of seconds become accessible. As this process is repeated for a number of cycles, with the cyclic activation analysis technique [31] the spectra from each counting cycle are summed together to give one final total spectrum. By means of this approach, a sufficient counting statistics and signal-to-background ratio for short-lived activation products of interest can be collected.

There are several isotopes of great interest for stellar nucleosynthesis studies that could be investigated with the CYCLING station. Some of them are stable nuclei, already known in certain neutron-energy ranges, and thus they will be measured at the beginning of the experimental campaign for benchmarking the performance of the CYCLING station in terms of accuracy and sensitivity. One such case is ^{19}F, whose neutron capture cross section is of great interest for understanding the origin of fluorine in the solar system [32]. Neutron capture on ^{19}F leads to the formation of ^{20}F with a half-life of only 11 s. Given the very small neutron capture cross section of only few mb in the keV energy range, and the short half-life of the product nucleus, these type of nuclei are excellent candidates for the cyclic activation technique. ^{19}F is copiously produced in AGB stars and an excess of ^{19}F has been observed in this type of stars [33], which motivated the measurement of this cross section at the $kT = 25$ keV quasi-stellar neutron spectrum of the Forschungszentrum Karlsruhe (FZK) using the cyclic-activation technique [34]. The MACS measured at 25 keV has an uncertainty of less than 3%, thus representing a good case for validating the performance of the CYCLING station. Once validated, it will become possible at CYCLING to extend the measurement of the ^{19}F MACS to other energy ranges of interest in AGB stars, for example at $kT \sim 8$ keV, which represents also a significant contribution to the destruction of ^{19}F in AGB stars [32].

From the astrophysics viewpoint, perhaps one of the most striking applications of the CYCLING station would be the possibility to directly access, for the first time, stellar (n, γ) measurements of relevance for the suggested intermediate neutron capture process (i process) [35]. The i process involves neutron captures at neutron densities of $10^{13} - 10^{16}$ cm^{-3}, in between the s and r processes. Recently, the i process attracted significant interest because it might explain the abundance pattern of a special kind of Carbon-Enhanced Metal-Poor stars (CEMPs), called CEMP-s/r [36]. From an experimental standpoint, the requirement of target-nuclei with short half-lives, such as some of those involved in the i

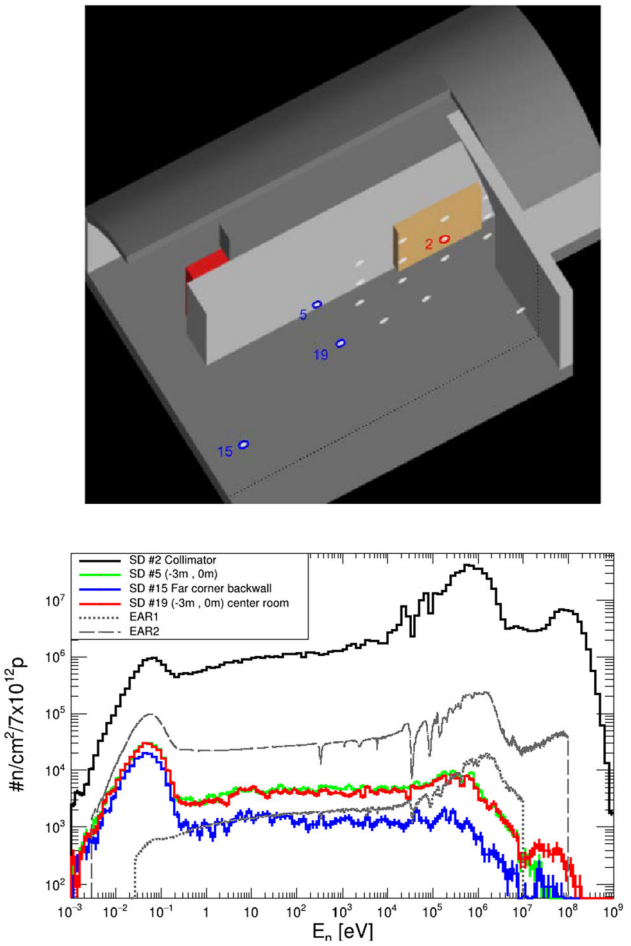

Fig. 14 Top: view of the a-NEAR bunker as implemented in GEANT4. Bottom: Simulated neutron flux of the n_TOF beam lines (EAR1/2 and a-NEAR) compared to the expected off-beam neutron flux registered in the highlighted scorers far from the a-NEAR beam

process, leading after neutron capture to product nuclei with even shorter half-lives, of the order of 1-100 s, offers a unique opportunity for combining in a synergetic fashion CYCLING with the nearby ISOLDE facility.

For example, it has been found that in the *i* process conditions variations in the neutron capture rates of some specific isotopes could affect the observable elemental ratio predictions involving Ba, La and Eu [37]. In this respect, some of the most relevant neutron-capture studies for future experiments at CYCLING could be [12]:

^{137}Cs($t_{1/2}$ = 30 y)$(n,\gamma)^{138}$Cs($t_{1/2}$ = 32.2 m) and
^{144}Ce($t_{1/2}$ = 285 d)$(n,\gamma)^{145}$Ce($t_{1/2}$ = 3 m).

A feasibility study is currently being performed for the CYCLING system at n_TOF, considering various factors. In principle, the time between consecutive proton pulses ($\geq$0.8 Hz), would provide periods of up to a few seconds without neutron beam, for decay counting. This condition is well suited for the measurement of the decay of very short-lived isotopes. However, a high-resolution γ-ray detector (e.g. HPGe) needs to be operated in the harsh radiation environment of the a-NEAR and thus the design of the measuring station poses a substantial challenge due its close proximity to the spallation target. In this context, an accurate knowledge of the expected neutron and γ-ray fields is a prerequisite for the feasibility of CYCLING. To this end, a first study has been carried out by means of Monte Carlo simulations of the expected off-beam neutron intensity at various positions inside the a-NEAR bunker (see top panel of Fig. 14). This simulations have been carried out with the GEANT4 toolkit (v10.6 p.03) using as primary particles the neutrons scored in the FLUKA simulations of Sect. 4. The average neutron flux per pulse at the collimator exit in a-NEAR is compared with three off-beam positions providing the lowest flux (blue dots in the Fig. 14). The comparison of the latter with the flux of the neutron beam in the first (EAR1) [38] and second (EAR2) [39] experimental areas at n_TOF indicates that the off-beam neutron flux at a-NEAR is in between the two. In contrast to the direct beam in a-NEAR, the off-beam spectra are dominated by back-scattered neutrons and feature an enhanced thermal component.

Following this simulation study, an experimental characterization of the neutron and γ-ray field in positions of interest for the design of the CYCLING station will be carried out, with different active and passive detectors [40]. The conclusions of these measurements will shed light on the background conditions of the a-NEAR and help in the optimization of the design of the beam dump and shielding elements that will facilitate the installation of the future CYCLING station.

6 Conclusions

The n_TOF experimental capability has recently been increased with the construction of a new high-flux experimental area for activation measurements. The new installation, called a-NEAR, exploits the extremely large neutron flux at 3 m from the n_TOF spallation target. The neutron beam enters the new station though a hole in the target shielding, in which a collimator system is inserted. Given the short distance from the target, the new station will be mostly dedicated to integral cross section measurements, either with the original neutron beam or with a moderated/filtered one, specifically designed to suitably shape the neutron spectrum. In particular, Monte Carlo simulations indicate that the use of neutron filters of different thickness allows one to obtain quasi-Maxwellian spectra of different thermal energies, to be used for challenging measurements of the MACS of short-lived isotopes of interest for nuclear astrophysics, with a reasonable uncertainty. The large flux and wide energy range of the neutron beam makes also feasible activation mea-

surements of interest for energy and medical applications. The a-NEAR station is complemented with a high-efficiency, low-background γ-ray and β-particle spectroscopy system, based on HPGe and scintillator detectors, positioned inside a dedicated room nearby the irradiation station. Future possibilities are now being investigated to perform fast-cycle irradiation-activation measurements inside a-NEAR, using an off-beam HPGe-based detection system. A first campaign for the commissioning of the neutron beam in the a-NEAR station has been performed, confirming the predictions of Monte Carlo simulations in terms of neutron flux, beam profile and background. The results of the commissioning will be reported in a forthcoming paper.

This work was supported by the Croatian Science Foundation under the project number HRZZ-IP-2022-10-3878. This project has received funding from the European Union's Horizon Europe Research and Innovation programme under Grant Agreement No 101057511. D. Rochman acknowledges support from EU APRENDE project, number 101164596. Support from the 401 funding agencies of all other participating institutes are gratefully acknowledged.

Funding Open access funding provided by CERN (European Organization for Nuclear Research).

Data Availability Statement This manuscript has no associated data. [Authors' comment: Data sharing not applicable to this article as no datasets were generated or analysed during the current study.]

Code Availability Statement This manuscript has no associated code/software. [Authors' comment: Code/Software sharing not applicable to this article as no code/software was generated or analysed during the current study.]

References

1. E.M. Burbidge, G.R. Burbidge, W.A. Fowler, F. Hoyle, Rev. Mod. Phys. **29**, 547 (1957). https://doi.org/10.1103/RevModPhys.29.547
2. A.G.W. Cameron, Astron. J. **62**, 9 (1957). https://doi.org/10.1086/107435
3. J.W. Truran, I. Iben Jr., Astrophys. J. **216**, 797 (1977). https://doi.org/10.1086/155523
4. S.A. Lamb, W.M. Howard, J.W. Truran, I. Iben Jr., Astrophys. J. **217**, 213 (1977). https://doi.org/10.1086/155571
5. A. Arcones, F.K. Thielemann, Astron. Astrophys. **31**(1), 1 (2023). https://doi.org/10.1007/s00159-022-00146-x
6. J.J. Cowan, C. Sneden, J.E. Lawler, A. Aprahamian, M. Wiescher, K. Langanke, G. Martínez-Pinedo, F.K. Thielemann, Rev. Mod. Phys. **93**(1), 015002 (2021). https://doi.org/10.1103/RevModPhys.93.015002
7. T. Kajino, W. Aoki, A.B. Balantekin, R. Diehl, M.A. Famiano, G.J. Mathews, Prog. Part. Nucl. Phys. **107**, 109 (2019). https://doi.org/10.1016/j.ppnp.2019.02.008
8. N. Nishimura, R. Hirschi, T. Rauscher, A.S.J. Murphy, G. Cescutti, Mon. Not. R. Astron. Soc. **469**(2), 1752 (2017). https://doi.org/10.1093/mnras/stx696
9. G. Cescutti, R. Hirschi, N. Nishimura, J.W. den Hartogh, T. Rauscher, A.S.J. Murphy, S. Cristallo, Mon. Not. R. Astron. Soc. **478**(3), 4101 (2018). https://doi.org/10.1093/mnras/sty1185
10. F. Käppeler, R. Gallino, S. Bisterzo, W. Aoki, Rev. Mod. Phys. **83**(1), 157 (2011). https://doi.org/10.1103/RevModPhys.83.157
11. I. Dillmann, O. Kester, R. Baartman, A. Chen, T. Junginger, F. Herwig, D. Kaltchev, A. Lennarz, T. Planche, C. Ruiz, N. Vassh, Eur. Phys. J. A **59**(5), 105 (2023). https://doi.org/10.1140/epja/s10050-023-01012-9
12. C. Domingo-Pardo, V. Babiano-Suarez, J. Balibrea-Correa, L. Caballero, I. Ladarescu, J. Lerendegui-Marco, J.L. Tain, A. Tarifeño-Saldivia, O. Aberle, V. Alcayne, S. Altieri, S. Amaducci, J. Andrzejewski, M. Bacak, C. Beltrami, S. Bennett, A.P. Bernardes, E. Berthoumieux, M. Boromiza, D. Bosnar, M. Caamaño, F. Calviño, M. Calviani, D. Cano-Ott, A. Casanovas, F. Cerutti, G. Cescutti, S. Chasapoglou, E. Chiaveri, N.M. Chiera, P. Colombetti, N. Colonna, P.C. Camprini, G. Cortés, M.A. Cortés-Giraldo, L. Cosentino, S. Cristallo, S. Dellmann, M. Di Castro, S. Di Maria, M. Diakaki, M. Dietz, R. Dressler, E. Dupont, I. Durán, Z. Eleme, S. Fargier, B. Fernández, B. Fernández-Domínguez, P. Finocchiaro, S. Fiore, F. García-Infantes, A. Gawlik-Ramięga, G. Gervino, S. Gilardoni, E. González-Romero, C. Guerrero, F. Gunsing, C. Gustavino, J. Heyse, W. Hillman, D.G. Jenkins, E. Jericha, A. Junghans, Y. Kadi, K. Kaperoni, F. Käppeler, G. Kaur, A. Kimura, I. Knapová, U. Köster, M. Kokkoris, M. Krtička, N. Kyritsis, C. Lederer-Woods, G. Lerner, A. Manna, T. Martínez, A. Masi, C. Massimi, P. Mastinu, M. Mastromarco, E.A. Maugeri, A. Mazzone, E. Mendoza, A. Mengoni, P.M. Milazzo, I. Mönch, R. Mucciola, F. Murtas, E. Musacchio-Gonzalez, A. Musumarra, A. Negret, A. Pérez de Rada, P. Pérez-Maroto, N. Patronis, J.A. Pavón-Rodríguez, M.G. Pellegriti, J. Perkowski, C. Petrone, E. Pirovano, J. Plaza, S. Pomp, I. Porras, J. Praena, J.M. Quesada, R. Reifarth, D. Rochman, Y. Romanets, C. Rubbia, A. Sánchez, M. Sabaté-Gilarte, P. Schillebeeckx, D. Schumann, A. Sekhar, A.G. Smith, N.V. Sosnin, M. Stamati, A. Sturniolo, G. Tagliente, D. Tarrío, P. Torres-Sánchez, J. Turko, S. Urlass, E. Vagena, S. Valenta, V. Variale, P. Vaz, G. Vecchio, D. Vescovi, V. Vlachoudis, R. Vlastou, T. Wallner, P.J. Woods, T. Wright, R. Zarrella, P. Žugec, (The n TOF Collaboration), Eur. Phys. J. A**59**(1), 8 (2023). https://doi.org/10.1140/epja/s10050-022-00876-7
13. N. Colonna, F. Belloni, E. Berthoumieux, M. Calviani, C. Domingo-Pardo, C. Guerrero, D. Karadimos, C. Lederer, C. Massimi, C. Paradela, R. Plag, J. Praena, R. Sarmento, Energy Environ. Sci. **3**, 1910 (2010). https://doi.org/10.1039/C0EE00108B
14. E. Morse, *Nuclear Fusion* (Springer, 2019)
15. M. Gilbert, S. Dudarev, S. Zheng, L. Packer, J.C. Sublet, Nucl. Fusion **52**(8), 083019 (2012). https://doi.org/10.1088/0029-5515/52/8/083019
16. R. Forrest, J. Kopecky, J.C. Sublet, UKAEA FUS 535 (2007)
17. W. Królas et al., Nucl. Fusion **61**(12), 125002 (2021). https://doi.org/10.1088/1741-4326/ac318f
18. N. Colonna et al., EPJ Web Conf. **165**, 01014 (2017). https://doi.org/10.1051/epjconf/201716501014

19. M. Ferrari et al., Phys. Rev. Accel. Beams **25**, 103001 (2022). https://doi.org/10.1103/PhysRevAccelBeams.25.103001
20. G. Gervino et al., Universe **8**(5), 255 (2022). https://doi.org/10.3390/universe8050255
21. R. Reifarth, M. Heil, C. Forssén, U. Besserer, A. Couture, S. Dababneh, L. Dörr, J. Görres, R. Haight, F. Käppeler, A. Mengoni, S. O'Brien, N. Patronis, R. Plag, R. Rundberg, M. Wiescher, J.B. Wilhelmy, Phys. Rev. C **77**, 015804 (2008). https://doi.org/10.1103/PhysRevC.77.015804
22. R. Esposito et al., Phys. Rev. Accel. Beams **24**, 093001 (2021). https://doi.org/10.1103/PhysRevAccelBeams.24.093001
23. The new n_TOF NEAR Station. https://cds.cern.ch/record/2737308/files/INTC-I-222.pdf. Accessed 7 Sept 2025
24. https://fluka.cern . Accessed 7 Sept 2025
25. C. Ahdida et al., Front. Phys. **9**, 788253 (2022). https://doi.org/10.3389/fphy.2021.788253
26. G. Battistoni et al., Ann. Nucl. Energy **82**, 10 (2015). https://doi.org/10.1016/j.anucene.2014.11.007
27. S. Urlass, A. Junghans, F. Mingrone, P. Peronnard, D. Stach, L. Tassan-Got, D. Weinberger, Nucl. Instrum. Methods Phys. Res. Sect. A Accel. Spectrom. Detectors Assoc. Equip. **1002**, 165297 (2021). https://doi.org/10.1016/j.nima.2021.165297, https://www.sciencedirect.com/science/article/pii/S0168900221002813
28. G. Feinberg, M. Paul, A. Arenshtam, D. Berkovits, D. Kijel, A. Nagler, I. Silverman, Nucl. Phys. A **827**(1), 590c (2009). https://doi.org/10.1016/j.nuclphysa.2009.05.130, https://www.sciencedirect.com/science/article/pii/S0375947409003960
29. R. Reifarth, L.P. Chau, M. Heil, F. Käppeler, O. Meusel, R. Plag, U. Ratzinger, A. Schempp, K. Volk, Publ. Astron. Soc. Austral. **26**(3), 255–258 (2009). https://doi.org/10.1071/AS08061
30. B. Fernández, M. Macías, C. Guerrero, M.A. Millán-Callado, T. Rodríguez-Gonzalez, J.M. Quesada, J. Gómez-Camacho, J. Praena, J. Phys: Conf. Ser. **1643**(1), 012033 (2020). https://doi.org/10.1088/1742-6596/1643/1/012033
31. H. Beer, G. Rupp, G. Walter, F. Voss, F. Käppeler, Nucl. Instrum. Methods Phys. Res. Sect. A Accel. Spectrom. Detectors Assoc. Equip. **337**(2), 492 (1994). https://doi.org/10.1016/0168-9002(94)91119-3
32. M. Forestini, S. Goriely, A. Jorissen, M. Arnould, Astron. Astrophys. **261**(1), 157 (1992). https://ui.adsabs.harvard.edu/abs/1992A&A...261..157F
33. A. Jorissen, V.V. Smith, D.L. Lambert, Astron. Astrophys. **261**, 164 (1992) https://ui.adsabs.harvard.edu/abs/1992A&A...261..164J
34. E. Uberseder, M. Heil, F. Käppeler, J. Görres, M. Wiescher, Phys. Rev. C **75**(3), 035801 (2007). https://doi.org/10.1103/PhysRevC.75.035801
35. J.J. Cowan, W.K. Rose, Astrophys. J. **212**, 149 (1977). https://doi.org/10.1086/155030
36. M. Hampel, R.J. Stancliffe, M. Lugaro, B.S. Meyer, Astrophys. J. **831**(2), 171 (2016). https://doi.org/10.3847/0004-637X/831/2/171
37. M.G. Bertolli, F. Herwig, M. Pignatari, T. Kawano, arXiv:1310.4578 (2013). Accessed 7 Sept 2025
38. M. Barbagallo et al., Eur. Phys. J. A **49**(12), 156 (2013). https://doi.org/10.1140/epja/i2013-13156-x
39. M. Sabaté-Gilarte et al., Eur. Phys. J. A **53**(10), 210 (2017). https://doi.org/10.1140/epja/i2017-12392-4
40. J. Lerendegui-Marco, et al., Measurement of the radiation background at the n_TOF NEAR facility to study the feasibility of cyclic activation experiments (2022). https://cds.cern.ch/record/2809131/files/INTC-I-241.pdf. Accessed 7 Sept 2025